J. Physiol. (1987), **384**, 199–222
With 10 text-figures
Printed in Great Britain

IDENTIFICATION OF SODIUM–CALCIUM EXCHANGE CURRENT IN SINGLE VENTRICULAR CELLS OF GUINEA-PIG

BY JUNKO KIMURA, SHUNICH MIYAMAE* AND AKINORI NOMA†

*From the National Institute for Physiological Sciences Myodaiji, Okazaki, 444, and *Department of Physiology, Kanazawa Medical University, Ishikawa-ken, 920-02, Japan*

(*Received 25 April 1986*)

SUMMARY

1. The Na–Ca exchange current was investigated in single ventricular cells from guinea-pig hearts by combining the techniques of whole-cell voltage clamp and intracellular perfusion.

2. The membrane conductance was minimized by blocking Ca and K channels as well as the Na–K pump. Under these conditions, when Ca^{2+} was loaded internally by a pipette solution containing 430 nM-Ca^{2+}, changing the Li^+-rich external solution to a Na^+-rich one induced a significant inward current. Applying external Na^+ in the absence of internal Ca^{2+} did not appreciably change the current.

3. In contrast, perfusing 1 mM-external Ca^{2+} in the presence of internal Na^+ which was loaded by a 20 mM-Na^+ pipette solution, induced a marked outward current. Ca^{2+} superfusion in the absence of internal Na^+ caused only a small current change.

4. The current–voltage relation of external-Ca^{2+}- and external-Na^+-induced current showed almost exponential voltage dependence as given by the equation $i = a \exp(rEF/RT)$, where a is a scaling factor that determines the magnitude of the current and r is a partition parameter used in the rate theory and represents the position of the energy barrier in the electrical field, which indicates the steepness of the voltage dependence of the current. E, F, R and T have their usual meanings. The value of a was 1–2 μA/μF and r about 0·35 for the Ca^{2+}-induced outward current. At very positive or negative potentials, the current magnitude became smaller than expected from an exponential relation.

5. The current was blocked by heavy metal cations, such as La^{3+}, Cd^{2+}, Mn^{2+} and Ni^{2+} and partially blocked by amiloride and D600.

6. The temperature coefficient (Q_{10}) value of the Ca^{2+}-induced outward current was $3{\cdot}6 \pm 0{\cdot}4$ ($n = 4$) at 0 mV and $4{\cdot}0 \pm 0{\cdot}9$ at 50 mV in the range between 21 and 36 °C.

7. The outward current magnitude showed a sigmoidal dependence upon the external Ca^{2+} concentration with a half-maximum concentration, $K_{\frac{1}{2}}$ of 1·38 mM and a Hill coefficient of $0{\cdot}9 \pm 0{\cdot}2$ ($n = 5$).

† Present address: Department of Physiology, Faculty of Medicine, Kyushu University, Fukuoka, 812 Japan.

8. Sr^{2+} could replace Ca^{2+} with $K_{\frac{1}{2}}$ of 7 mM. Mg^{2+} and Ba^{2+}, however, did not replace Ca^{2+}.

9. The inward current component also showed a sigmoidal external Na^+ dependence with $K_{\frac{1}{2}}$ of $87{\cdot}5 \pm 10{\cdot}7$ mM and a Hill coefficient of $2{\cdot}9 \pm 0{\cdot}4$ ($n = 6$).

10. The reversal potential of the current was obtained near the values expected for 3 Na^+:1 Ca^{2+} exchange.

11. The Ca^{2+}- and Na^+-induced currents decayed transiently. This phenomenon is most likely caused by Ca^{2+} concentration change immediately under the membrane.

12. The above findings largely agree with the properties of the Na–Ca exchange studied by ionic flux measurements in squid axon and cardiac sarcolemmal vesicles. Thus we conclude that the Na^+- and Ca^{2+}-induced currents were generated by electrogenic Na–Ca exchange.

INTRODUCTION

The free Ca^{2+} concentration within the cardiac cell is maintained 10^3–10^4 times lower than the outside as is the case in various other tissues. This requires a powerful Ca^{2+} extrusion system in the membrane where two such mechanisms are known (Sulakhe & St. Louis, 1980). One is the Na–Ca exchange mechanism and the other the ATP-dependent Ca pump. The latter saturates at a lower Ca^{2+} concentration and has a smaller transport rate than the former and thus during cardiac activity the Na–Ca exchanger may play a major role in expelling Ca^{2+} (Caroni & Carafoli, 1981).

The cardiac Na–Ca exchange mechanism was first demonstrated experimentally in guinea-pig atria by Reuter & Seitz in 1968. They showed external Na^+-dependent ^{45}Ca efflux and subsequently Glitsch, Reuter & Scholz (1970) reported internal Na^+-dependent Ca^{2+} influx so that a concept of bidirectional Na–Ca exchange mechanism was established. Similar systems were also found in crab nerve (Baker & Blaustein, 1968), squid axons (Baker, Blaustein, Hodgkin & Steinhart, 1969) and in various other tissues and animals (for review see Campbell, 1983).

It was Blaustein & Hodgkin (1969) who demonstrated that in cyanide-poisoned squid axons the energy source of the Na–Ca exchange is the electrochemical potential gradient of both Na^+ and Ca^{2+} across the membrane. Furthermore, they suggested that the stoicheiometry is 3 or more Na^+ to 1 Ca^{2+} and thus the system is likely to be electrogenic. Various workers have thereafter investigated the properties of the Na–Ca exchange system by the radioactive ionic flux method in squid axons (see review by Dipolo & Beaugé, 1983), cardiac membrane vesicles (see review by Philipson, 1985) and in intact cardiac strands (reviewed by Langer, 1982). The accumulated results indicated that the stoicheiometry is most probably 3 Na^+:1 Ca^{2+} and so the system is electrogenic. If such a membrane current is detected, we will be able to measure directly the Ca^{2+} efflux during cardiac activity. Although various workers had tried to demonstrate the exchange current, the results were rather obscure because it was difficult to separate the exchange current from various other membrane currents (for review see Eisner & Lederer, 1985).

Recent development of the single-cell voltage-clamp technique and internal perfusion of the patch pipette (Soejima & Noma, 1984) have made it possible to

control the internal ionic environment. This method allows isolation of a current by blocking most other membrane currents by appropriate blockers from inside and outside (Matsuda & Noma, 1984; Gadsby, Kimura & Noma, 1985). Using this method we have recently found an outward current which is activated by the presence of Na^+ inside and Ca^{2+} outside the membrane and is inhibited by La^{3+} (Kimura, Miyamae & Noma, 1986*a*; Kimura, Noma & Irisawa, 1986*b*). The current is not activated when internal Ca^{2+} is completely chelated by a high concentration of EGTA. These results strongly suggested that it is generated by the electrogenic Na–Ca exchange mechanism. In the present report, we further investigate the current with regard to its voltage dependence, ionic selectivity and its sensitivity to various blocking agents and temperatures.

METHODS

Preparation of the cells

Single ventricular cells of guinea-pig were prepared by a method similar to that described by Taniguchi, Kokubun, Noma & Irisawa (1981). Briefly the heart was perfused with Ca^{2+}-free Tyrode solution containing collagenase (20 mg/50 ml) for 30–40 min on a Langendorff apparatus. The digested heart was stored in low-Cl, high-K medium in the refrigerator. Before each experiment a small piece of the ventricular tissue was dissected out and shaken in the recording chamber to disperse the cells. The input capacitance of the cells varied between 120 and 350 pF.

Voltage-clamp technique

The intracellular perfusion technique has been described in detail in other papers published from our laboratory (Soejima & Noma, 1984; Sato, Noma, Kurachi & Irisawa, 1985). Whole-cell clamp was performed according to the original technique developed by Hamill, Marty, Neher, Sakmann & Sigworth (1981). In the clamp circuit, an input resistance of 100 MΩ was used and series resistance compensation was included. Either square or ramp clamp pulses were employed. The shape of the ramp pulse was of three phases: an initial 90 mV depolarizing phase from the holding potential of −30 mV, a second hyperpolarization of 180 mV and then a third phase returning to the holding potential at a speed of ±90 mV/0·5–1 s. The current–voltage (*I–V*) curve was measured during the second hyperpolarizing portion.

Solutions

The compositions of the external solutions are as follows. The normal Tyrode solution contained (in mM): NaCl, 136·9; KCl, 5·4; $CaCl_2$, 1·8; $MgCl_2$, 0·5; NaH_2PO_4, 0·33; glucose, 5; HEPES, 5 (pH = 7·4 with NaOH). The Na^+ external solution contained (in mM): NaCl, 140; $MgCl_2$, 2; HEPES, 5 (pH = 7·4 with LiOH). For the Li^+ external solution, NaCl was replaced by equimolar LiCl and $CaCl_2$ was added if necessary. The Cs^+-rich internal solution contained (in mM): CsOH, 166; aspartic acid, 42; EGTA, 42; MgATP, 10; K_2creatinephosphate (CrP), 5; $MgCl_2$, 3; and HEPES, 5 (pH = 7·4 with CsOH). Na^+-rich internal solution containing 100 mM-Na^+ instead of Cs^+ was made and was mixed with the Cs^+-rich solution to obtain a desired concentration of Na^+. As blockers in the external solution, ouabain (Sigma) (20 μM) was used to block the Na–K pump, $BaCl_2$ (1 mM) and CsCl (2 mM) to block K channels and D600 (2 μM) to block Ca channels. In the internal solution, 20 mM-tetraethylammonium chloride (TEA) was also included to block K channels. In the presence of these blockers time-dependent currents were mostly blocked and the remaining conductance showed a linear *I–V* relation. To pevent the cell from contracture caused by Ca^{2+} entering in exchange for Na^+, 42 mM-EGTA was put in the pipette solution so that the buffering capacity for Ca^{2+} was increased. The currents in general did not show any significant difference at concentrations between 42 mM- and 5 mM-EGTA in the internal solution. The concentration of free internal Ca^{2+} was adjusted by adding $CaCl_2$ to the internal solution, which was calculated by using Fabiato & Fabiato's equations (1979) with a correction by Tsien & Rink (1980). The stability constants for ATP, and CrP were according to Fabiato (1981) and those for EGTA were from Schwarzenbach, Senn & Anderegg (1957). As a result, the following combinations were used: pCa 7·2 (free

Ca^{2+} 67 nM = 42 mM-EGTA + 21 mM-Ca), pCa 6·7 (free Ca^{2+} 172 nM = 42 mM-EGTA + 30 mM-Ca) and pCa 6·4 (free Ca^{2+} 430 nM = 42 mM-EGTA + 36 mM-Ca).

The external solutions were heated by a water jacket before entering the recording chamber. The temperature of the bath solution was measured near the cell using a small thermistor. All experiments were performed at 34–36 °C unless otherwise stated.

Drug

Amiloride was a generous gift from Merck Sharp Company, Rahway, NJ, U.S.A.

RESULTS

Membrane currents generated by the presence of Na^+ and Ca^{2+} on either side of the membrane

The Na^+-dependent Ca^{2+} flux or the Ca^{2+}-dependent Na^+ flux has been ascribed to a Na–Ca exchange mechanism (Reuter & Seitz, 1968; Glitsch *et al.* 1970; Blaustein & Russell, 1975). If a membrane current is detected under analogous conditions to these flux experiments, it can be attributed to the electrogenic Na–Ca exchange. Thus if 3 or more Na^+ are exchanged for 1 Ca^{2+}, an outward membrane current should be evoked by applying external Ca^{2+} in the presence of internal Na^+, and an inward current by applying external Na^+ in the presence of internal Ca^{2+}. Application of these ions, however, may also induce other changes on the membrane current. These possibilities were tested in the following experiments.

(*a*) *External-Na^+-induced inward current in internal-Ca^{2+}-loaded cells.* The external solution was changed briefly from 140 mM-Li^+ to 140 mM-Na^+ at first in the absence of internal Ca^{2+} and then again after loading internal Ca^{2+} by 430 mM-Ca^{2+} pipette solution (Fig. 1*A*). Li^+ is used as a control because it is known to substitute very little for Na^+ in the exchange mechanism (Baker, 1972; Kadoma, Froehlich, Reeves & Sutko, 1982; Ledvora & Hegyvary, 1983). The internal solution contained no Na^+ and the external solution contained 1 mM-external Ca^{2+}. The first Na^+ application did not change the current at −30 mV but the second one induced a large inward shift of the holding current which decayed after a peak. *I–V* relations obtained by ramp pulses before and during the first external Na^+ superfusion were completely superimposable (Fig. 1*Ba* and *b*).

Loading Ca^{2+} in the cell always increased the membrane conductance (Fig. 1*Bc*), suggesting that there is a Ca^{2+}-sensitive background conductance. The *I–V* curve of this Ca^{2+}-sensitive component crossed with the control before loading Ca^{2+} at −30–0 mV, indicating that this component may pass through a non-specific cation channel described by Colquhoun, Neher, Reuter & Stevens (1981). Yellen (1982) found a similar channel in neuroblastoma and reported that the conductance was similar for Na^+ and Li^+. We call this component a Ca^{2+}-sensitive background current which is not analysed in detail in the present study.

The *I–V* relations obtained before and during the second external Na^+ perfusion in the presence of internal Ca^{2+} are shown in Fig. 1*C* and *D*. The external-Na^+-induced current was inward initially at the potentials negative to about +30 mV and as the current magnitude became larger, it was inward at all potentials with respect to the control current (Fig. 1*C*). The current showed a voltage dependence and was larger at more negative potentials. The *I–V* relation of the difference current will be shown

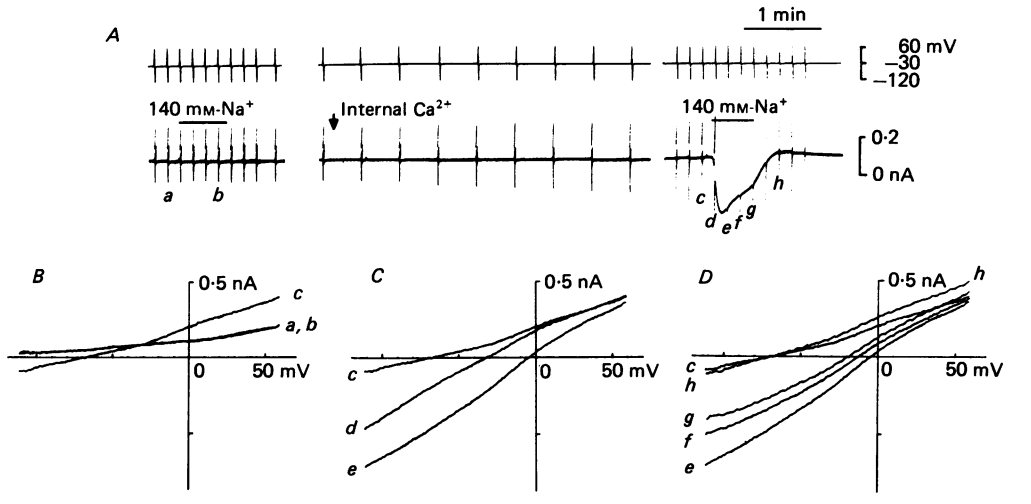

Fig. 1. *A*, chart record of voltage (top) and current (bottom) at the holding potential of −30 mV. Ramp pulses of ±90 mV/0·5–1 s were given every 10 or 20 s. The external solution was changed from 140 mM-Li^+ to 140 mM-Na^+ for a period indicated above the current trace in the absence of internal Ca^{2+} (left) and after loading internal Ca^{2+} by 430 nM-Ca^{2+} in the pipette solution (right). External Ca^{2+} is 1 mM throughout. The intervals between the panels are 3 min on the left and 1 min on the right. The current traces indicated by *a–h* are shown in *B–D*. *B*, *I–V* relations obtained at *a* in external Li^+ and *b* in external Na^+ in the absence of internal Ca^{2+} and at *c* in external Li^+ in the presence of internal Ca^{2+}. *C*, *I–V* curves before (*c*) and during (*d* and *e*) the onset of external-Na^+-induced current. *D*, *I–V* relations after the peak of external-Na^+-induced current (*e–g*). *h* is obtained at the peak of overshoot of the holding current after washing off external Na^+. The capacitance of the cells was 203 pF.

in Fig. 8. After the peak, the current magnitude became smaller (Fig. 1*D*). On removing external Na^+, the current moved outward before returning to the control level (Fig. 1*Dh*). If the Ca^{2+}-sensitive background current does not discriminate between Na^+ and Li^+ as is the case shown by Yellen (1982), the Na^+-induced inward current is very likely attributed to Na–Ca exchange current. The origin of the transient decay of the current after the peak and an outward current overshoot on washing off external Na^+ will be investigated in the later section.

(*b*) *External-Ca^{2+}-dependent outward current in internal-Na^+-loaded cells.* Since Na–Ca exchange is bidirectional, an outward component of the Na–Ca exchange current should be induced by perfusing external Ca^{2+} in the presence of internal Na^+. For this purpose, the external solution consisted of 140 mM-Li^+ without Na^+ and nominally free Ca^{2+} for the control while 1 mM-Ca^{2+} for the test solution. Ba^{2+} (1 mM) was added to prevent the membrane from becoming leaky by eliminating all the external divalent cations from the control solution. The internal solution contained 30 mM-Na^+ and also 67 nM-free Ca^{2+} (pCa 7·2), since it is known that the Na–Ca exchange does not operate in the absence of internal Ca^{2+} (Baker & McNaughton, 1976; Allen & Baker, 1985; see also Kimura *et al.* 1986*b*).

As shown in the inset of Fig. 2*A*, 1 mM-external Ca^{2+} was perfused in the absence of internal Na^+ as a control. The *I–V* curve was shifted slightly outward by external

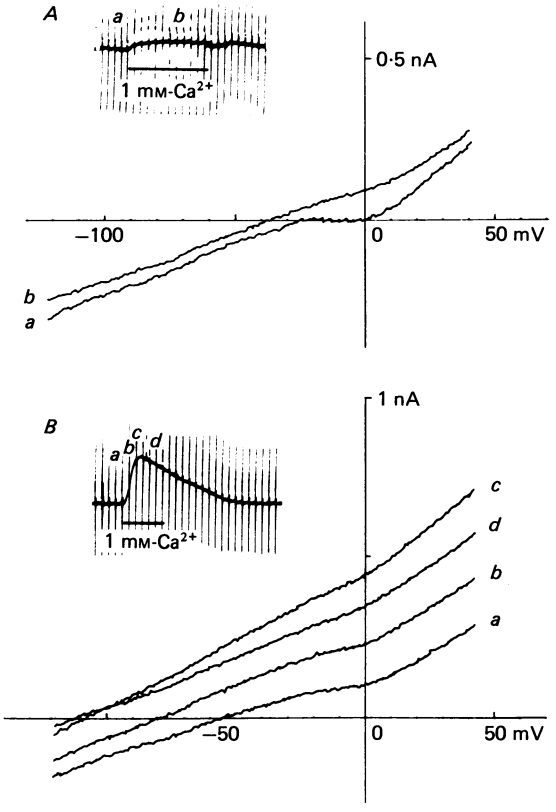

Fig. 2. *A*, *I–V* relations taken before (*a*) and during (*b*) 1 mM-external Ca^{2+} perfusion in the absence of internal Na^+. The external solution contains 140 mM-Li^+ and no Na^+. The inset indicates the chart record of the current at −30 mV with the regular ramp pulses every 5 s. *B*, *I–V* relations obtained before applying external Ca^{2+} (*a*), during the onset (*b* and *c*) and the decay of the external Ca^{2+}-(1 mM) induced current (*d*) in the presence of 30 mM-Na^+ in the pipette solution. The capacitance of the cell was 180 pF.

Ca^{2+} (Fig. 2*Ab*). In this case, an inward deflexion is seen in the control *I–V* curve at around 0 mV which is most likely because the Ca channel was not yet fully blocked by D600 and probably Ba^{2+} was passing through. After washing out external Ca^{2+}, Na^+ was loaded by changing the internal solution to one containing 30 mM-Na^+. An increase in internal Na^+ usually slightly increased the membrane conductance (compare Fig. 2*Aa* and *Ba*, see also Kimura *et al.* 1986*b*, Fig. 1). Perfusing 1 mM-external Ca^{2+} then induced a significant outward current (Fig. 2*B* inset). It decayed transiently after reaching a peak and disappeared when external Ca^{2+} was washed off, which occurred slowly in this case since the inflow of the control solution to the bath was slow.

The *I–V* curves obtained by ramp pulses during the Ca^{2+} superfusion are illustrated in Fig. 2*B*. The current was outward with respect to the control at all potentials investigated and became larger at more positive potentials in a similar manner but in the opposite direction to the inward current shown in Fig. 1. Therefore it is likely that this outward current and the above inward current are of the same entity and that these currents are generated by the electrogenic exchange of Na^+ and Ca^{2+}.

I–V relation of Na^+- and Ca^{2+}-sensitive current under physiological conditions

To investigate the *I–V* relations of the Na^+- and Ca^{2+}-induced current, it may be better to do so near its reversal potential, since the current may either saturate or be modified in the voltage range far away from this. If the Na–Ca exchange is driven by the electrochemical potential gradients of Na^+ and Ca^{2+}, the reversal potential is expressed by the following equation (Mullins, 1981):

$$E_{NaCa} = (nE_{Na} - 2E_{Ca})/(n-2), \quad (1)$$

where E_{NaCa} is the reversal potential of i_{NaCa}, E_{Na} and E_{Ca} the equilibrium potentials for Na^+ and Ca^{2+} respectively and n is the stoicheiometry for Na^+. Supposing a stoicheiometry of 3 Na^+:1 Ca^{2+}, the reversal potential is given by:

$$E_{NaCa} = 3\,E_{Na} - 2\,E_{Ca}. \quad (2)$$

Under ionic conditions close to physiological ones such as 140 mM-external Na^+, 20 mM-internal Na^+, 67 nM-internal Ca^{2+}, the values of E_{NaCa} at 1 mM- and 2 mM-external Ca^{2+} are -100 mV and -119 mV respectively. If current reversal can be demonstrated at these potentials, it will be a strong evidence for Na–Ca exchange current. Furthermore we will be able to estimate the physiological *I–V* relation of the Na–Ca exchange current.

To make internal Ca^{2+} and Na^+ concentrations as close as possible to those in the pipette solution, the clamp was held in the control solution containing 0·1 mM-external Ca^{2+} at -30 mV which is close to E_{NaCa} of -39 mV at 0·1 mM-external Ca^{2+}. As shown in the inset of Fig. 3*A*, changing external Ca^{2+} from 0·1 to 1 mM induced a marked outward current. The *I–V* curves in Fig. 3*A* were obtained in control (*a*) and at an early stage of the peak shift of the holding current (*b*). The two *I–V* curves, *a* and *b*, nearly cross in the very negative potential range. Similar results were also obtained when 2 mM-external Ca^{2+} was perfused in the bath. The control current (*a*) in 0·1 mM-Ca^{2+} might have contained a small fraction of inward i_{NaCa} at around -100 mV thus preventing E_{NaCa} from appearing. This hypothesis is tested by using a model equation in the Discussion.

Fig. 3*B* shows the difference current obtained by subtracting the control in 0·1 mM-Ca^{2+} from the *I–V* curve in 1 mM. This current turned out to have an exponential voltage dependence which is revealed by a semilogarithmic plot shown in Fig. 3*C*. For quantification the difference current was fitted by the following simple equation (Noble, 1986, see also DiFrancesco & Noble, 1985):

$$i = a \exp(rEF/RT), \quad (3)$$

where a is a scaling factor that determines the magnitude of the current and r is a partition parameter used in the rate theory and represents the position of the energy barrier in the electrical field, which indicates the steepness of the voltage dependence of the current. E, F, R and T have their usual meanings. The value of a was obtained from the current magnitude at 0 mV in Fig. 3*B* and r from the slope in Fig. 3*C*. In this case, the value of a was 1·16 μA/μF at 1 mM-external Ca^{2+} and r was 0·38. On average, a was $0{\cdot}83 \pm 0{\cdot}25$ μA/μF ($n = 7$) at 1 mM-external Ca^{2+} and $1{\cdot}66 \pm 0{\cdot}39$ μA/μF ($n = 4$) at 2 mM-external Ca^{2+}, indicating that the current density

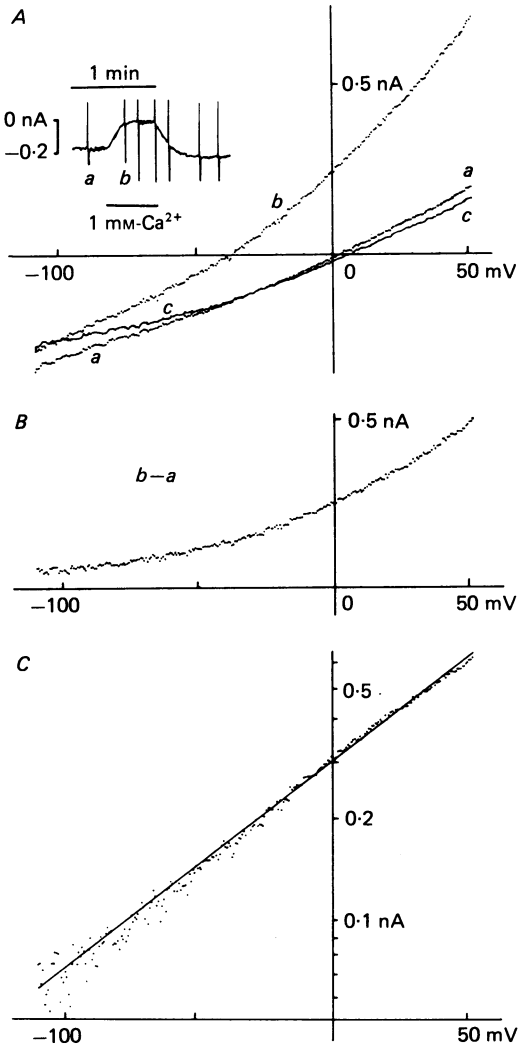

Fig. 3. *A*, *I–V* relations measured in the presence of 140 mM-external Na^+, 20 mM-internal Na^+, and 67 nM-internal Ca^{2+}. The *I–V* curve (*a*) was in 0·1 mM-external Ca^{2+} (control) and (*b*) in 1 mM-external Ca^{2+} test solution. The inset shows where *a* and *b* were taken during the development of the current by increasing external Ca^{2+}. The current (*c*) which is crossing with *b* at about −100 mV is a background current obtained by eqn. (3) as described in the Discussion. *B*, the difference current between *a* in 0·1 mM- and *b* in 1 mM-external Ca^{2+}. *C*, exponential plot of the difference current in *B*. The slope of the regression line is 0·32. The capacitance of the cell was 215 pF.

is proportional to external Ca^{2+} concentration. An average value of r was $0{\cdot}36 \pm 0{\cdot}03$ ($n = 6$) at 1 mM-external Ca^{2+} and $0{\cdot}34 \pm 0{\cdot}02$ ($n = 4$) at 2 mM-external Ca^{2+} as shown in Table 1. The value of r is smaller than 0·5, suggesting that the *I–V* curve is not symmetrical between outward and inward components. The exponential *I–V* relation may well indicate that this current is a carrier-mediated Na–Ca exchange current.

TABLE 1. Parameters of the Ca^{2+}-activated current

Cell no.	r	a (μA/μF)	i_{NaCa} (nA)	E_{NaCa} (mV)	C_m (pF)
		1 mM-Ca^{2+}			
1	0·35	1·21	0·26	−92	215
1	0·38	1·16	0·25	−98	215
2	0·32	0·76	0·30	−98	402
3	0·32	0·78	0·31	−103	395
4	0·41	0·82	0·13	−80	158
5	0·39	0·60	0·07	−100	117
6	0·35	0·47	0·19	−95	398
Mean	0·36	0·83	0·22	−95	271
±S.D.	±0·03	±0·25	±0·09	±7	±123
		2 mM-Ca^{2+}			
4	0·31	1·96	0·31	−92	158
4	0·36	2·09	0·33	−98	158
5	0·36	1·11	0·13	−110	117
6	0·33	1·46	0·58	−100	398
Mean	0·34	1·66	0·34	−100	207
±S.D.	±0·02	±0·39	±0·19	±8	±128

r, the partition parameter; a, the proportional factor in eqn. (3); i_{NaCa}, the magnitude of the current at 0 mV, and E_{NaCa}, the reversal potential obtained by using a model described in the Discussion. C_m, the membrane capacitance which was obtained by $C_m = i_c(dV/dt)^{-1}$ where i_c was calculated by the current jump at the turning point between descending and ascending portions of the ramp pulse. The duplicated cell number indicates repeated experiments in the same cell. The ionic conditions are 140 mM-external Na^+, 20 mM-internal Na^+ and 67 nM-Ca^{2+} in the pipette.

Blockers of the current

Various multivalent cations, such as La^{3+} and Mn^{2+}, are reported to inhibit the Na–Ca exchange in membrane vesicles or multicellular preparations of the heart as well as in squid axons (see review by Eisner & Lederer, 1985). It was tested whether the above current was blocked by these chemicals. The heavy metal cations, such as La^{3+} (0·5 mM), Cd^{2+} (1 mM), Mn^{2+} (1 mM) and Ni^{2+} (5 mM) all blocked the current, most of them reversibly. The blocking effect of La^{3+} has already been described in the previous report (Kimura *et al.* 1986*b*). Among these cations Ni^{2+} appeared to inhibit the current fairly selectively with little effect on the background current. Fig. 4 shows the block of the Ca^{2+}-induced current with 1, 2 and 5 mM-Ni^{2+}. It can be seen that the membrane conductance in 0·1 mM-external Ca^{2+} was slightly decreased by 1 mM-Ni^{2+}. Application of 2 mM-Ca^{2+} in the presence of Ni^{2+} activated a progressively smaller current as the concentration of Ni^{2+} was progressively increased. After washing off Ni^{2+}, the amplitude of the Ca^{2+}-induced current almost completely restored.

The Ca^{2+}-induced current was also sensitive to D600 and amiloride (Siegl, Cragoe, Trumble & Kaczorowski, 1984). D600 (22 μM) depressed the current by about 65 % of the control but a low dose of 2 μM, which is sufficient to block the Ca channel, did

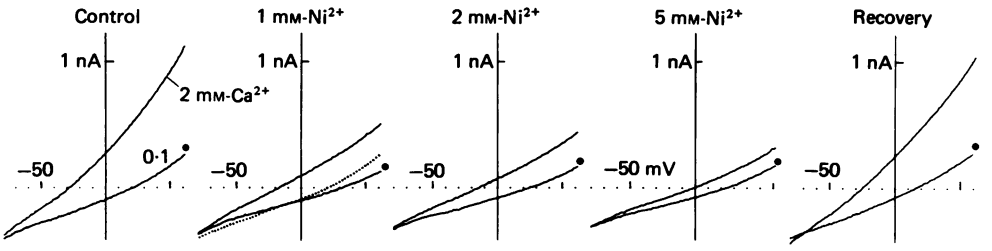

Fig. 4. Blocking effect of 1, 2 and 5 mM-Ni^{2+}. Ionic conditions are 140 mM-external Na^+, 20 mM-internal Na^+ and 67 nM-internal Ca^{2+}. Control I–V curves in 2 mM- and 0·1 mM-external Ca^{2+} (filled circles) are shown on the first panel from the left. The middle three panels indicate 1, 2 and 5 mM-Ni^{2+} and the last panel shows the recovery at 10 min after washing off 5 mM-Ni^{2+}. Dotted curve in the second panel is a superimposed control in 0·1 mM-Ca^{2+} before applying 1 mM-Ni^{2+}.

not seem to have any effect. Amiloride (3 mM) also blocked the current by about 25 %. Higher amounts of amiloride, however, affected the background current. These results indicate that the major portion, if not all, of the Ca^{2+}- and Na^+-induced current is elicited by electrogenic Na–Ca exchange.

Temperature sensitivity of the Ca^{2+}-induced outward current

The temperature coefficient, Q_{10}, of the Na–Ca exchange current is expected to be higher than that of an ionic channel current, which is typically between 1·3 and 1·6 (Hille, 1984). To obtain the Q_{10} value, the Ca^{2+}-induced outward current was activated by applying 1 mM-external Ca^{2+} repeatedly while lowering the temperature of the external solution from 36 to 20 °C. The ionic conditions are the same as above (140 mM-external Na^+, 20 mM-internal Na^+ and 67 nM-internal Ca^{2+}). Fig. 5*A* represents the I–V curves at three different temperatures in the same cell. The current magnitude was measured at 50 and 0 mV where the non-selective background current is supposed to be least contaminating. The difference current magnitude at 0 mV between the control (0·1 mM-Ca^{2+}) and 1 mM-external Ca^{2+} was plotted in Fig. 5*B*. The results in four different cells revealed that the current was extremely temperature sensitive. The average Q_{10} value between 36 and 21 °C was $3{\cdot}6 \pm 0{\cdot}4$ ($n = 4$) at 0 mV and $4{\cdot}0 \pm 0{\cdot}9$ at +50 mV. These values at two different potentials are not significantly different.

Previous workers have reported smaller values; i.e. 2·3 (Blaustein & Hodgkin, 1969), 2·7 (Baker *et al.* 1969) in squid axon, 1·35 in guinea-pig atria (Reuter & Seitz, 1968) and ~ 1·4 in dog Purkinje fibres (Coraboeuf, Gautier & Guiraudou, 1981). Russell & Blaustein (1974) reported a value of 3·7 in squid axon which is consistent with our result. The precise value of the Q_{10}, however, may depend on the exact ionic conditions and membrane potential. As the conditions are changed so may the rate-limiting reaction and thence the Q_{10}. The Q_{10} values that we found are significantly higher than that of an ionic channel current, and thus support the hypothesis that the current is due to Na–Ca exchange.

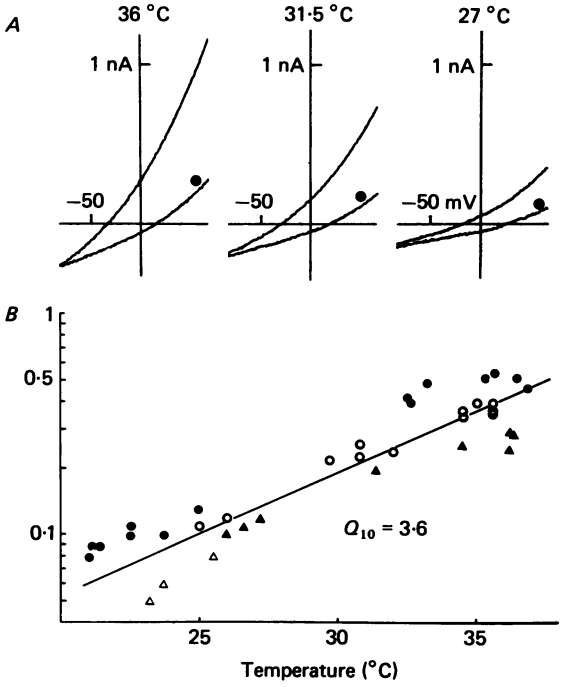

Fig. 5. Effect of temperature. The ionic conditions are the same as in Fig. 4. *A*, representative current traces at 0·1 mM-external Ca^{2+} (control; filled circles) and at 1 mM-external Ca^{2+} at three different temperatures indicated above each panel. *B*, the difference in current amplitude at 0 mV in 1 and in 0·1 mM-external Ca^{2+} was measured at each temperature and plotted semilogarithmically against the temperature for four different cells. Different symbols indicate different cells.

External Ca^{2+} dependence of the current

Ca^{2+} dependence of the current was investigated by measuring the outward current at different concentrations of external Ca^{2+}. The control external solution contained no Ca^{2+} but 0·1 mM-EGTA and 1 mM-Ba^{2+}. As shown in Fig. 6*A*, when the concentration of external Ca^{2+} was progressively increased from 0·1 to 20 mM, the magnitude of the external-Ca^{2+}-induced outward current became progressively larger. The decay of the current after the peak also became more prominent in higher concentrations of external Ca^{2+} and so did the undershoot on washing off Ca^{2+}. This decay of the current may be due to accumulation of Ca^{2+} immediately under the membrane, which will be discussed in a later section. The control *I–V* curve obtained before the Ca^{2+} application (not shown) was subtracted from that at the peak response and the difference *I–V* curves were superimposed in Fig. 6*B*. All the difference *I–V* curves appear to be almost exponential.

The dose–response relationship to Ca^{2+} was obtained by plotting the current semilogarithmically against external Ca^{2+} concentration (Fig. 6*C*). The current magnitude was measured at +50 mV where the Na–Ca exchange component is substantially larger than the background conductance, so that the contamination of the background current could be minimized. As seen in Fig. 6*C*, the current saturated

at higher external Ca^{2+} concentrations and the dose–response relation was almost sigmoid with the half-maximum Ca^{2+} concentration ($K_{\frac{1}{2}}$) at about 1·2 mM. The Hill plot gave a coefficient of about 1. In five experiments the average Hill coefficient was $0{\cdot}9 \pm 0{\cdot}2$ and $K_{\frac{1}{2}}$ was 1·38 mM.

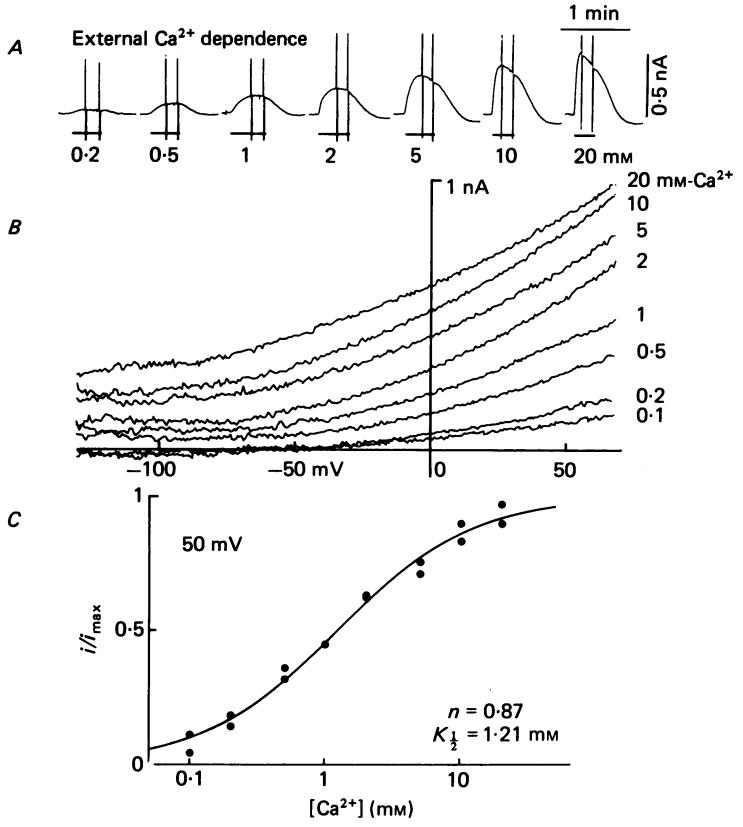

Fig. 6. *A*, current records on changing external Ca^{2+} from nominally free to various concentrations indicated below each trace between 0·2 and 20 mM. The holding potential is −30 mV. *B*, *I–V* relations obtained by the difference between the peak of the activation (taken by the first ramp pulse on each trace in *A*) and control (not shown) for each trace. Ca^{2+} concentrations are indicated on the right of each trace. *C*, dose–response relation of the current at +50 mV. Current magnitude at each external Ca^{2+} concentration in *B* was normalized with reference to the current at 20 mM-external Ca^{2+} (i/i_{max}) and plotted against external Ca^{2+} concentrations semilogarithmically. The inset indicates the Hill coefficient of 0·87 and the half-maximum ($K_{\frac{1}{2}}$) external Ca^{2+} concentration of 1·21 mM.

In most experiments, the $K_{\frac{1}{2}}$ value shifted to the left by 1 mM at 0 mV compared to that at +50 mV. This shift could be explained by the following model for example. At 0 mV the rate-limiting step may be the efflux of Na^+ whereas this step will be accelerated at +50 mV and may no longer be rate limiting. It is therefore possible that the availability of external Ca^{2+} is considerably more limiting at +50 mV and thus a higher $K_{\frac{1}{2}}$ value is obtained.

Dependence of the current on other divalent cations

Whether other divalent cations such as Ba^{2+}, Mg^{2+} and Sr^{2+} could replace external Ca^{2+} in the exchange was tested using a pipette solution containing 20 mM-Na^+ and 67 nM-Ca^{2+}. The external application of Mg^{2+} instead of Ca^{2+} scarcely changed the *I–V* curve. When Ba^{2+} of 2–10 mM was applied in the presence of 0·1 mM-Ca^{2+} in the bath solution, the slope conductance of the *I–V* curve was reduced in a dose-dependent manner and the curves crossed at around −10 mV, indicating that Ba^{2+} blocked a non-specific ionic conductance (Figure not shown). These findings indicate that Mg^{2+} and Ba^{2+} cannot replace Ca^{2+} in the Na–Ca exchanger. In contrast, Sr^{2+} could substitute for Ca^{2+} as observed by other workers (Tibbits & Philipson, 1982; Yau & Nakatani, 1984).

Fig. 7*A* shows the effect of different concentrations of Sr^{2+} from 1 to 20 mM investigated in a similar manner as was done for Ca^{2+}. The current magnitude became larger as the Sr^{2+} concentration became higher. The Sr^{2+}-induced current decayed after the peak more rapidly than the Ca^{2+}-induced current (Fig. 6*A*) and an undershoot after washing off external Sr^{2+} was more prominent than that of the latter. The *I–V* relations obtained by subtracting the control *I–V* curve from the one at the peak of each response are shown in Fig. 7*B*. The *I–V* curves in different Sr^{2+} concentrations were almost exponential but unlike those for Ca^{2+} they crossed with the voltage axis at around −50 mV. These results may be because Sr^{2+} which entered the cell in exchange for Na^+ accumulated more readily than Ca^{2+} under the membrane, since the stability constant of EGTA is smaller for Sr^{2+} than for Ca^{2+} by more than three orders (8·5 M^{-1} for the former and 11 M^{-1} for the latter). It can be calculated by eqn. (1) that an increase in intracellular divalent cations shifts the reversal potential of the exchange current in a positive direction. In addition, the Ca^{2+}-sensitive background conductance which has a reversal potential near 0 mV may have also increased by accumulated Sr^{2+} and have resulted in the apparent current reversal. In Fig. 7*C*, the dose–response relation was measured at +60 mV. The Hill coefficient was 1·1 and the $K_{\frac{1}{2}}$ was about 6 mM, indicating that one molecule of Sr^{2+} binds to the exchanger like Ca^{2+} and that the affinity of Sr^{2+} is smaller than Ca^{2+}.

Na^+ dependence of the current

Na^+ dependence of the inward current component was investigated by changing external Na^+ concentrations in internal-Ca^{2+}-loaded cells. A representative case in Fig. 8 is the same cell as shown in Fig. 1 where the pipette solution contained 430 nM-Ca^{2+} without internal Na^+. The control external solution contained 140 mM-Li^+ and 1 mM-Ca^{2+} and the clamp was held at −30 mV. When Li^+ external solution was changed into one containing progressively smaller concentrations of Na^+ from 140 mM to 17·5 mM, an inward current of progressively smaller magnitude developed (Fig. 8*A*). The *I–V* curves of the Na^+-induced currents were measured by the difference between before and at the peak effect of the Na^+ superfusion. As shown in Fig. 8*B*, the *I–V* curve became less steep as external Na^+ was decreased. The *I–V* curves developed exponentially at positive potentials but as the potential became more negative to about −30 mV, they deviated from an exponential relation as if

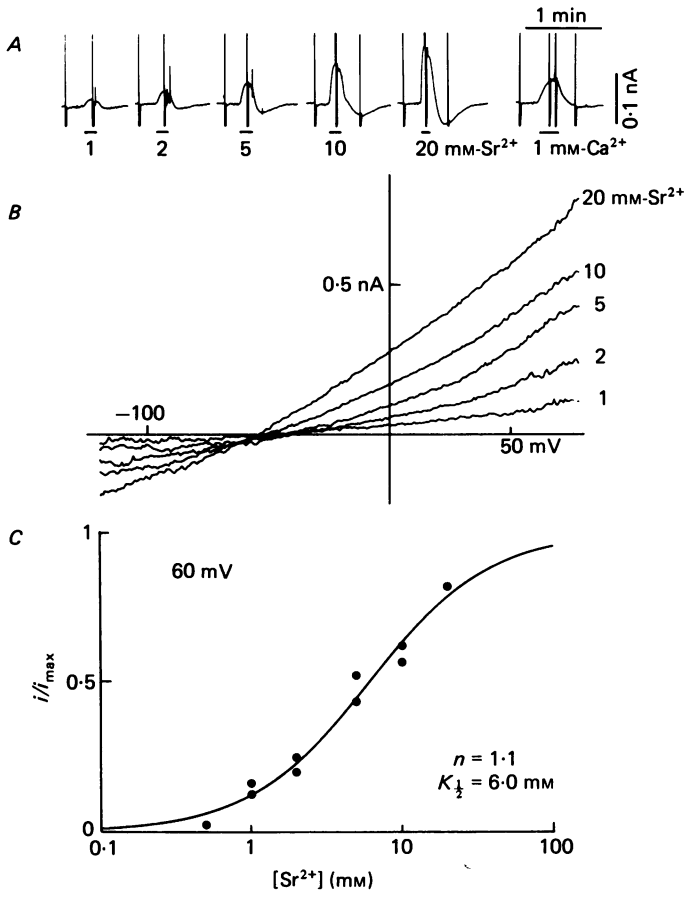

Fig. 7. *A*, current records at various concentrations of external Sr^{2+} indicated below each trace. On the left end of the panel the current activated by 1 mM-external Ca^{2+} in the same cell is shown for comparison. 140 mM-external Na^+, 20 mM-internal Na^+ and 67 nM-internal Ca^{2+}. *B*, the difference between the currents in the presence and absence of external Sr^{2+} were plotted against voltage. Numerals at the right of each curve give Sr^{2+} concentrations in mM. *C*, current magnitudes at +60 mV at each concentration of Sr^{2+} in *B* were normalized referring to the current magnitude at 20 mM and plotted against external Sr^{2+} concentrations semilogarithmically. The inset indicates the Hill coefficient of 1·1 and the half-maximum ($K_{\frac{1}{2}}$) Sr^{2+} concentration of 6·0 mM.

the currents began to saturate. The current magnitude measured at −100 mV was plotted semilogarithmically against Na^+ concentration, which showed almost sigmoidal dependence on external Na^+ (Fig. 8*C*). If $K_{\frac{1}{2}}$ was 70 mM, a straight line was obtained in the Hill plot and a Hill coefficient became 3. In six experiments the mean value of the Hill coefficient was 2·9±0·4 and $K_{\frac{1}{2}}$ was 87·5±10·7 mM. This result is consistent with the 3 Na^+:1 Ca^{2+} stoicheiometry. The deviation of the *I–V* curve from exponentials may be caused by internal Ca^{2+} depletion.

Reversal potential of the Ca^{2+}-induced current

Since 5 mM-Ni^{2+} was found to block the Ca^{2+}-induced current without much effect on the background current, it was used to measure the reversal potential of the

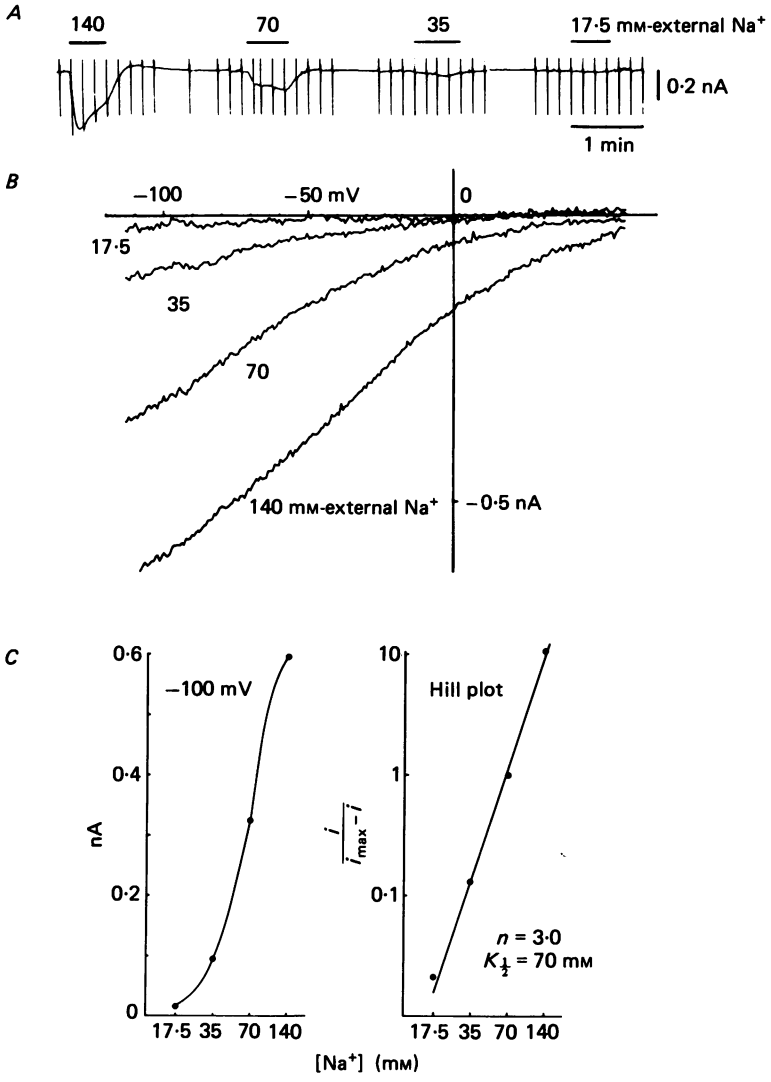

Fig. 8. *A*, chart record of applying various concentrations of external Na^+. Control ionic conditions are 140 mM-Li^+, 0 internal Na^+, 1 mM-external Ca^{2+} and 430 nM-internal Ca^{2+}. Test external Na^+ concentrations are illustrated at the top of the bars which indicate the duration of Na^+ superfusion. *B*, the difference currents between the peak activation and the control in 140 mM-external Li^+ before applying external Na^+ were plotted against voltage. *C*, left: the current magnitudes were plotted against the logarithm of external Na^+ concentrations. Right: Hill plot of the current in *C*. A straight line was obtained at a half-maximum concentration ($K_{\frac{1}{2}}$) of 70 mM-external Na^+ in this case and the slope (Hill coefficient) was 3.

Ca^{2+}-induced current. If the current reverses at the expected value of E_{NaCa}, it can be identified as the exchange current. Although 5 mM-Ni^{2+} sometimes does not block the Ca^{2+} current completely but by about 80%, this would not affect E_{NaCa}. Under conditions of 140 mM-external Na^+, 10 mM-internal Na^+ and 172 nM-internal Ca^{2+}, E_{NaCa} at 1, 2 and 4 mM-external Ca^{2+} will be −20, −39 and −57 mV respectively

according to eqn. (2). The clamp was held at −35 mV in the presence of 2 mM-external Ca^{2+}. Then external Ca^{2+} was changed from 2 mM to 1 mM or 4 mM and finally 5 mM-Ni^{2+} was added with 2 mM-external Ca^{2+} to obtain the control current. Fig. 9*A* shows the *I–V* curves recorded in 1 and 4 mM-external Ca^{2+} and in 2 mM-external Ca^{2+} together with 5 mM-Ni^{2+} in the bath solution. The *I–V* curves were shifted in the negative direction by increasing external Ca^{2+} as expected. The difference currents

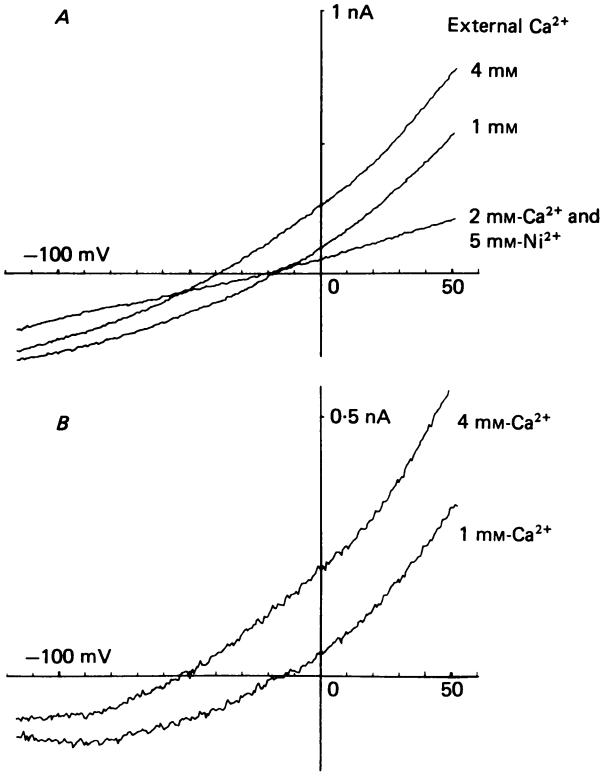

Fig. 9. *A*, *I–V* curves obtained at 4 mM, 1 mM-external Ca^{2+} and 2 mM-Ca^{2+} with 5 mM-Ni^{2+} in the presence of 140 mM-external Na^+, 10 mM-internal Na^+ and 172 nM-internal Ca^{2+}. The clamp was held at −35 mV and external Ca^{2+} was changed from 2 to 1 mM, 4 mM, or to 2 mM-Ca^{2+} with 5 mM-Ni^{2+}. *I–V* curves were obtained by ramp pulses. *B*, to see the reversal potentials, the difference currents were obtained by subtracting the current in 5 mM-Ni^{2+} from the *I–V* curves at 4 and 1 mM-Ca^{2+}. The reversal potential for 4 mM-Ca^{2+} can be seen at −53 mV and at −15 mV for 2 mM-Ca^{2+}.

between each external Ca^{2+} and the control in Ni^{2+} are shown in Fig. 9*B*. The currents showed reversal potentials at about −13 mV in 1 mM-external Ca^{2+}, −25 mV in 2 mM-external Ca^{2+} (Figure not shown) and −53 mV at 4 mM-external Ca^{2+}. These values are strikingly close to the expected values. In six experiments the mean values obtained in the above method were -17 ± 10 mV at 1 mM, -24 ± 8 mV at 2 mM and -42 ± 12 mV at 4 mM-external Ca^{2+}. These values are significantly different from those expected by 4:1 stoicheiometry, i.e. +24, +15 and +6 mV, respectively. These results indicate that this current is the Na–Ca exchange current with a stoicheiometry of 3:1.

Analysis of the current decay

When a large current was activated by superfusing Na^+ or Ca^{2+}, it usually decayed after a peak even though the test solution was still flowing. On washing off the test solution the holding current showed a rebound before returning to the control level (see Figs. 1*A* and Fig. 6*A*). A similar phenomenon was observed when voltage jumps were given while activating the Ca^{2+}-induced current (Fig. 10). Although a short

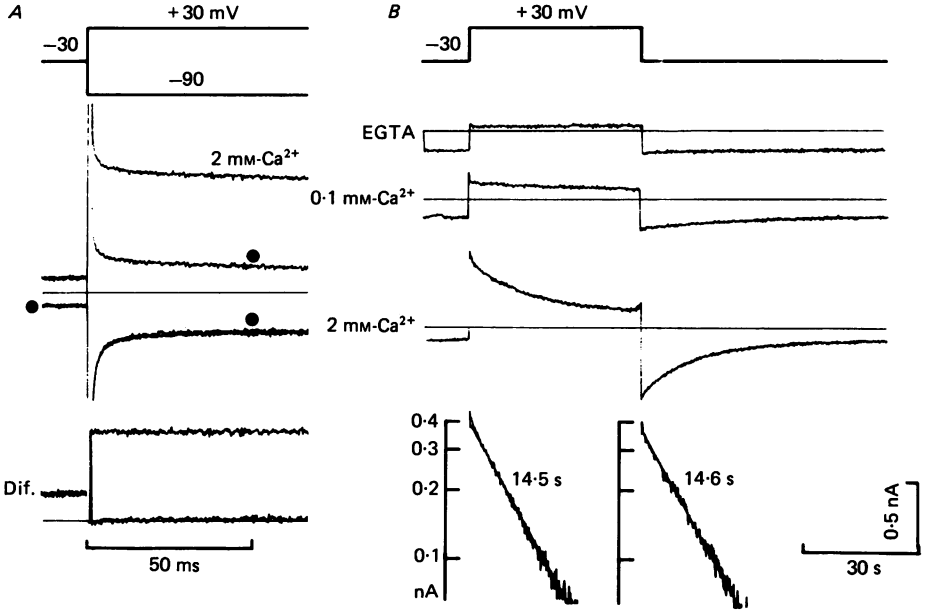

Fig. 10. Current traces during a short period of about 70 ms (*A*) and a long period of 45 s (*B*) of square clamp pulse in various external Ca^{2+} concentrations. The top of each column illustrates clamp pulses with voltages indicated. The middle column shows currents in response to above voltages in EGTA without external Ca^{2+} (indicated by filled circles in *A*) and 0·1 mM (*B*) and/or 2 mM-external Ca^{2+} (*A* and *B*). Zero current level is indicated in each trace. *A*, at −90 mV currents in the absence and presence of external Ca^{2+} are completely superimposable. At the bottom the difference currents between the presence and absence of Ca^{2+} at two different potentials do not show any time-dependent change. *B*, current traces in 2 mM-external Ca^{2+} show prominent time-dependent decay both on depolarization and repolarization. At the bottom, exponential fits of the current decay on depolarization (left) and on repolarization (right) in 2 mM-Ca^{2+} are shown with the regression line. The time constant of the decay on depolarization was 14·5 s and 14·6 s on repolarization. 140 mM-external Na^+, 20 mM-internal Na^+ and 67 nM-internal Ca^{2+} are present.

depolaring clamp pulse of 300 ms did not induce any obvious time-dependent current (Fig. 10*A*), prolongation of the pulse to 45 s revealed a prominent decay of the current on both depolarization and hyperpolarization (Fig. 10*B*). In the absence of external Ca^{2+} such changes were not observed and the decay was tiny when external Ca^{2+} concentration was low. The time course of the current decay fitted well a single exponential with similar time constants on depolarization by 60 mV and on repolarization, as indicated at the bottom of Fig. 10*B*. The average of six experiments gave time constants of $10{\cdot}7 \pm 3{\cdot}8$ s on depolarization by 40–60 mV and $12{\cdot}2 \pm 2{\cdot}1$ s on repolarization.

There are two possibilities which explain this phenomenon. One is the intrinsic property of the carrier and the other a secondary phenomenon most probably due to Ca^{2+} accumulation under the membrane in the case of the decay of the outward current or depletion in the case of the inward current. The following three findings support the second possibility. (1) The Sr^{2+}-induced current decayed faster than the Ca^{2+}-induced one during the voltage jumps as described previously. (2) When intracellular EGTA concentration was decreased to 2 mM, the decay of the current became faster (Figure not shown). The time constants of the decay in 2 mM-EGTA was 7·4 s and in 42 mM-EGTA, 11·5 s in the same cell. (3) The time constant of the decay was smaller at higher Ca^{2+} concentrations, namely 16·4, 12·0, 7·2 and 6·5 s at 0·5, 2, 5 and 10 mM-external Ca^{2+}, respectively.

Preliminary experiments using 10 mM-BAPTA (1,2-bis(*o*-aminophenoxy)ethane-*N*,*N*,-*N*′,*N*′-tetraacetic acid) another Ca^{2+} chelator which does not affect pH and chelates Ca^{2+} faster than does EGTA (Tsien, 1980), considerably reduced the decay of the outward current. Thus the cause of the current decay may be multifold. A large amount of Ca^{2+} entering accumulated transiently under the membrane. As a result, the Na–Ca exchange *I–V* relation must have shifted in the positive direction, and thus caused the apparent decay of the current. Meanwhile as the Ca^{2+} was progressively chelated, proton release from EGTA might have acidified the cell interior, which could have inhibited pH sensitive Na–Ca exchange current. Intracellular acidosis is also known to be produced by an increase in internal Ca^{2+} in the absence of EGTA (Vaughan-Jones, Lederer & Eisner, 1983). Accumulated Ca^{2+} may have also increased the Ca^{2+}-sensitive background current which could in addition cause the decay phenomenon.

It might be noted that the inward current (Fig. 1) also decays. This current is presumably associated with a decrease of internal Ca^{2+} and therefore is unlikely to produce an intracellular acidosis. The decaying current on the voltage jump was completely depressed by 5 mM-Ni^{2+}. These results indicate that the major component of the decaying current was due to the Na–Ca exchange.

DISCUSSION

The membrane current investigated above had the following characteristics which led us to conclude that the current is generated by the Na–Ca exchange mechanism. (1) An inward current was elicited by internal Ca^{2+} and external Na^+ and an outward current by external Ca^{2+} and internal Na^+. (2) The *I–V* relation was exponential and the magnitude of the current was Na^+- and Ca^{2+}-dependent. (3) The current had a Q_{10} value of 3·6–4 which was larger than that of channel currents. (4) Sr^{2+} but not Mg^{2+} nor Ba^{2+} could replace Ca^{2+}. (5) The current was blocked by La^{3+}, Mn^{2+}, Cd^{2+} and Ni^{2+}, and partly by D600, and amiloride. (6) The reversal potential was seen at potentials very close to the thermodynamically expected values for 3 Na^+:1 Ca^{2+} stoicheiometry. (7) The current was not activated in the absence of internal Ca^{2+} (Kimura *et al.* 1986*b*). In the following paragraphs, we will compare some of these properties with those of Na–Ca exchange in squid axons and cardiac vesicles.

The voltage dependence of Na–Ca exchange was also observed in the radioactive tracer measurements. External-Na^+-dependent $^{45}Ca^{2+}$ efflux was reduced by mem-

brane depolarization and increased by hyperpolarization in squid axons (Blaustein, Russell & De Weer, 1974; Mullins & Brinley, 1975; Dipolo, Bezanilla, Caputo & Rojas, 1985) and in bovine cardiac vesicles (Reeves & Hale, 1984). In squid axons 25 mV hyperpolarization in the membrane potential caused 1·3–2·1-fold increase in Na^+-dependent Ca^{2+} efflux (Mullins & Brinley, 1975; Dipolo *et al.* 1985). Blaustein *et al.* (1974, Fig. 5) also obtained results in which the flux decrease was smaller than e-fold for 25 mV depolarization, although they expected an e-fold change/25 mV, since the flux rate was thought to be proportional to $\exp(EF/RT)$. Recently Noble (1986) introduced a partition parameter (r) of Eyring rate theory to the exchange current so that the current is expressed as a function of $\exp(rEF)$ (see eqn. (3)). If r is 0·5, the exchange rate is symmetrical between inward and outward directions. According to this concept, the change of 1·3–2·1-fold/25 mV in Ca^{2+} efflux corresponds to the r (or rather $1-r$ for the direction of Ca^{2+} efflux) value of 0·26–0·74.

In our hands the value of r is about 0·35 for the outward exchange current (Ca^{2+} influx). If the energy barrier for the exchange senses a single unit of charge during each transfer, then the parameter for inward i_{NaCa} should be $1-r$, that is 0·65. Some results indicated that this is so. The inward currents in Fig. 1*C*, for example, showed an almost exponential *I–V* relation at the potentials positive to about −30 mV which could be fitted with a value of $1-r$ close to 0·65. Although the value of r varied with different ionic concentrations, it was always smaller than 0·5 for the outward exchange current. These results indicate that the exchange current is asymmetrical between the inward and outward components and that the inward component (Ca^{2+} efflux) is more steeply voltage dependent than the outward component (Ca^{2+} influx).

The stoicheiometry of 3 Na^+:1 Ca^{2+} determined from the reversal potential was consistent with the Hill coefficient for Na^+ of 2·9 ($n = 6$) and for Ca^{2+} of 0·9 ($n = 4$). Some workers have raised the possibility of 4:1 on theoretical ground (Mullins, 1979) and experimentally in dog heart vesicles (Ledvora & Hegyvary, 1983). More results, however, supported a 3:1 ratio (in squid axons, Blaustein *et al.* 1974; Blaustein & Santiago, 1977; in cardiac sarcolemmal vesicles, Pitts, 1979; Reeves & Hale, 1984, and in the rabbit heart, Bridge & Bassingthwaighte, 1983). The values close to 3:1 were also obtained in sheep Purkinje fibres using ion-sensitive electrodes (2·5–2·6:1, Sheu & Fozzard, 1982; 2·5–2·9:1, Bers & Ellis, 1982).

Our $K_{\frac{1}{2}}$ values for Ca^{2+} (1·2 mM) and Na^+ (90 mM) are similar to those obtained in squid axons ($K_{\frac{1}{2}(Na)} \sim 75$ mM and $K_{\frac{1}{2}(Ca)} \sim 2$ mM or $K_{\frac{1}{2}}$ (Na) 125 mM and $K_{\frac{1}{2}(Ca)}$ 3 mM), crab nerve ($K_{\frac{1}{2}(Na)}$ 75 mM and $K_{\frac{1}{2}(Ca)}$ 2 mM) and in barnacle muscles ($K_{\frac{1}{2}(Na)}$ 60 mM) (see Table III, Blaustein *et al.* 1974). These values, however, are much larger than those obtained in cardiac vesicles where the Michaelis constant, K_m (Ca) is 15–40 μM or even 1–2 μM (see review, Philipson, 1985). This discrepancy may originate, as Philipson (1985) has suggested, from the difference in ionic environment. In the vesicles, one side of the membrane is exposed only to Ca^{2+} and the other side only to Na^+. If Na^+ and Ca^{2+} compete for the binding sites as suggested by other workers (Reeves & Sutko, 1983), it may be reasonable that under our ionic conditions, where Na^+ and Ca^{2+} are both present, the K_m value for Ca^{2+} becomes larger. The same argument is possible for Na^+ for which a K_m value of 7–32 mM in vesicles has been reported (Philipson, 1985).

E_{NaCa} obtained by using a model of i_{NaCa}

Since the Na–Ca exchange current has been found to have a simple exponential relation to voltage near the reversal potential, we used the model of Noble (1986; see also DiFrancesco & Noble, 1985) for simulating the experiment shown in Fig. 3 and obtaining a reversal potential of the exchange current. The following is the equation:

$$i_{NaCa} = k\{(\text{internal Na})^3\,(\text{external Ca})\exp((n-2)\,rEF/RT) - (\text{external Na})^3\,(\text{internal Ca})\exp(-(n-2)\,(1-r)\,EF/RT)\}, \quad (4)$$

where k, in this case, is a scaling factor and other parameters are the same as those in eqns. (1) and (3). This model is based on the assumption that the carrier normally moves only when it can bind both ions so that only two possible voltage-dependent processes are taken account of: the movement when transporting Na^+ inwards and the movement when transporting Na^+ outwards.

If we tentatively assume that k is constant at different external Ca^{2+} of 1 mM and 0·1 mM, the difference current (i_{dif}) will be given as the following simple exponential function:

$$i_{dif} = k\,(\text{internal Na})^3\,(1\ \text{mM-external Ca} - 0{\cdot}1\ \text{mM-external Ca})\exp(rEF/RT). \quad (5)$$

The experimental difference current shown in Fig. 3*B* fitted well with eqn. (5) with the values of $k = 2{\cdot}07 \times 10^{-5}\ \mu A/mM^4 . \mu F$ and $r = 0{\cdot}38$. i_{NaCa} in 0·1 mM-external Ca^{2+} was obtained by inserting the values of r and k and the ionic concentrations to eqn. (4). It was then subtracted from the control *I–V* curve and the resulting background current was drawn on Fig. 3*Ac*. The background current crossed with the current in 1 mM-external Ca^{2+} at −98 mV. This value was strikingly close to the E_{NaCa} of −100 mV for 3:1 stoicheiometry, but far from that of −18 mV for 4:1. As shown in Table 1, the simulation of ten cases gave average values of k and E_{NaCa}, $5{\cdot}94 \pm 2{\cdot}74 \times 10^{-5}\ \mu A/mM^4 . \mu F$ and -95 ± 7 mV at 1 mM-external Ca^{2+} and in four cases at 2 mM-external Ca^{2+}, $6{\cdot}28 \pm 3{\cdot}57 \times 10^{-5}\ \mu A/mM^4 . \mu F$ and -100 mV ± 8 mV respectively. Although E_{NaCa} at 2 mM-Ca^{2+} did not shift to an expected value of −119 mV (cf. −28 mV for 4:1 stoicheiometry), it was obtained at a slightly more negative potential than that at 1 mM-Ca^{2+}. Thus this model appears to fit our experimental data very well. It was, however, found that the *I–V* curve of this current is not always exponential but it deviates as if it saturates at the potentials far away from the reversal potential. This is not unexpected, since there is likely to be some maximal rate for the movement of the carriers. We hope that our experiment will be able to provide information on limitation of the carrier reaction to be incorporated in this model.

Na–Ca exchange current during action potentials

The above model may allow us to estimate i_{NaCa} during action potentials. According to aequorin luminescence studies in dog Purkinje fibres, intracellular Ca^{2+} rises as the action potential is initiated and then it falls to the original low level during the plateau phase (Wier & Isenberg, 1982). This fall in internal Ca^{2+} may be partly due to Ca^{2+} uptake by the sarcoplasmic reticulum and partly to Ca^{2+} extrusion by

Na–Ca exchange. If so, Na–Ca exchange may expel Ca^{2+} most vigorously during the plateau phase. If the maximum activity of internal Ca^{2+} is 1 μM (Fabiato & Baumgarten, 1984) and an activity coefficient of Ca^{2+} 0·33, internal Ca^{2+} concentration increases to 3 μM during the action potential. Incorporating this value into eqn. (4) together with ionic conditions of 140 mM-external Na^+, 10 mM-internal Na^+, 2 mM-external Ca^{2+} and the average values of r and k at 2 mM-external Ca^{2+} as stated above, i_{NaCa} of $-0{\cdot}5$ $\mu A/\mu F$ is obtained at +10 mV of the plateau potential. This current magnitude corresponds to Ca^{2+} efflux of 50 μmol/l.s, assuming a volume of a ventricular cell as 20 pl. With this rate of efflux it will take 200 ms to expel 10 μM-Ca^{2+} entered through the Ca channel, which is roughly estimated by Fabiato *et al.* (1984). This assumption does not contradict aequorin signal transients so much.

Resting internal Ca^{2+} concentration measured by ion-sensitive electrodes is 270 nM in guinea-pig ventricle (Coray & McGuigan, 1981). At this internal Ca^{2+} concentration, i_{NaCa} of $-0{\cdot}035$ $\mu A/\mu F$ (3·6 μmol/l.s) is calculated to flow at the resting potential of −85 mV. If, however, Na–Ca exchange is equilibrated at the resting potential of −85 mV, then intracellular Ca^{2+} can be calculated as 33 nM. These assumptions indicate how much i_{NaCa} varies depending on internal Ca^{2+} and the membrane potential. To know an exact amount of i_{NaCa} flowing during cardiac activity, we need more accurate information on internal Ca^{2+} concentration dynamics.

The transient inward current (i_{ti}) is known to develop under Ca^{2+} overload in cardiac cells (see review, Eisner & Lederer, 1985). The origin of this current has not yet been elucidated but it has been attributed to the Na–Ca exchange current and/or to the Ca^{2+}-activated non-specific cation conductance (Kass, Lederer, Tsien & Weingart, 1978). Recent reports by Arlock & Katzung (1985) and Brown, Noble, Noble & Taupignon (1986) have demonstrated that i_{ti} disappears on replacing Na^+ by Li^+. Our present results also support a possibility that a considerable part of i_{ti} is carried by i_{NaCa}.

We thank Professor H. Irisawa for stimulating discussions and helpful advice, Professor D. Noble for kind advice and providing us his preprint manuscripts, Dr H. Matsuda for comments on the manuscript and Dr H. Brown for correcting the English. This work was supported by grants from Ministry of Education, Science and Culture, and Ministry of Health and Welfare of Japan. J.K. was a fellow of The Japan Society for the Promotion of Science.

REFERENCES

ALLEN, T. J. A. & BAKER, P. F. (1985). Intracellular Ca indicator Quin-2 inhibits Ca^{2+} inflow via Na_i/Ca_o exchange in squid axon. *Nature* **315**, 755–756.

ARLOCK, P. & KATZUNG, B. G. (1985). Effects of sodium substitutes on transient inward current and tension in guinea-pig and ferret papillary muscle. *Journal of Physiology* **360**, 105–120.

BAKER, P. F. (1972). Transport and metabolism of calcium ions in nerve. *Progress in Biophysics and Molecular Biology* **24**, 177–223.

BAKER, P. F. & BLAUSTEIN, M. P. (1968). Sodium-dependent uptake of calcium by crab nerve. *Biochimica et biophysica acta* **150**, 167.

BAKER, P. F., BLAUSTEIN, M. P., HODGKIN, A. L. & STEINHARDT, R. A. (1969). The influence of calcium on sodium efflux in squid axons. *Journal of Physiology* **200**, 431–458.

BAKER, P. F. & MCNAUGHTON, P. A. (1976). Kinetics and energetics of calcium efflux from intact squid giant axons. *Journal of Physiology* **259**, 103–144.

BERS, D. M. & ELLIS, D. (1982). Intracellular calcium and sodium activity in sheep heart Purkinje fibres. Effects of changes of external sodium and intracellular pH. *Pflügers Archiv* **393**, 171–178.

BLAUSTEIN, M. P. & HODGKIN, A. L. (1969). The effect of cyanide on the efflux of calcium from squid axons. *Journal of Physiology* **200**, 497–527.

BLAUSTEIN, M. P. & RUSSELL, J. M. (1975). Sodium–calcium exchange and calcium–calcium exchange in internally dialyzed squid giant axons. *Journal of Membrane Biology* **22**, 285–312.

BLAUSTEIN, M. P., RUSSELL, J. M. & DE WEER, P. (1974). Calcium efflux from internally dialyzed squid axons: the influence of external and internal cations. *Journal of Supramolecular Structure* **2**, 558–581.

BLAUSTEIN, M. P. & SANTIAGO, E. M. (1977). Effects of internal and external cations and of ATP on sodium–calcium and calcium–calcium exchange in squid axons. *Biophysical Journal* **20**, 79–111.

BRIDGE, J. H. B. & BASSINGTHWAIGHTE, J. B. (1983). Uphill sodium transport driven by an inward calcium gradient in heart muscle. *Science* **219**, 178–180.

BROWN, H. F., NOBLE, D., NOBLE, S. J. & TAUPIGNON, A. I. (1986). Relationship between the transient inward current and slow inward currents in the sino-atrial node of the rabbit. *Journal of Physiology* **370**, 299–315.

CAMPBELL, A. K. (1983). *Intracellular Calcium*. Chichester: Wiley.

CARONI, P. & CARAFOLI, E. (1981). The Ca^{2+}-pumping ATPase of heart sarcolemma. *Journal of Biological Chemistry* **256**, 3263–3270.

COLQUHOUN, D., NEHER, E., REUTER, H. & STEVENS, C. S. (1981). Inward current channels activated by intracellular Ca in cultured heart cells. *Nature* **294**, 752–754.

CORABOEUF, E., GAUTIER, P. & GUIRAUDOU, P. (1981). Potential and tension changes induced by sodium removal in dog Purkinje fibres: role of an electrogenic sodium–calcium exchange. *Journal of Physiology* **311**, 605–622.

CORAY, A. & MCGUIGAN, J. A. S. (1981). Measurement of intracellular ionic calcium concentration in guinea pig papillary muscle. In *Ion Selective Microelectrodes and Their Use in Excitable Tissues*, ed. SYKOVA, E., HINK, P. & VYKLICKY, L., pp. 299–301. New York: Plenum.

DIFRANCESCO, D. & NOBLE, D. (1985). A model of cardiac electrical activity incorporating ionic pumps and concentration changes. *Philosophical Transactions of the Royal Society B* **307**, 353–398.

DIPOLO, R. & BEAUGÉ, L. (1983). The calcium pump and sodium–calcium exchange in squid axons. *Annual Review of Physiology* **45**, 313–324.

DIPOLO, R., BEZANILLA, F., CAPUTO, C. & ROJAS, H. (1985). Voltage dependence of the Na/Ca exchange in voltage-clamped, dialyzed squid axons. *Journal of General Physiology* **86**, 457–478.

EISNER, D. A. & LEDERER, W. J. (1985). Na–Ca exchange: stoichiometry and electrogenicity. *American Journal of Physiology* **248**, C189–202.

FABIATO, A. (1981). Myoplasmic free calcium concentration reached during the twitch of an intact isolated cardiac cell and during calcium-induced release of calcium from the sarcoplasmic reticulum of a skinned cardiac cell from the adult rat or rabbit ventricle. *Journal of General Physiology* **78**, 457–497.

FABIATO, A. & BAUMGARTEN, C. M. (1984). Methods for detecting calcium release from the sarcoplasmic reticulum of skinned cardiac cells and the relationship between calculated trans-sarcolemmal calcium movements and calcium release. In *Physiology and Pathophysiology of the Heart*, ed. SPERELAKIS, N., pp. 215–254. The Hague: Martinus Nijhoff.

FABIATO, A. & FABIATO, F. (1979). Calculator programs for computing the composition of the solutions containing multiple metals and ligands used for experiments in skinned muscle cells. *Journal de physiologie* **75**, 463–505.

GADSBY, D. C., KIMURA, J. & NOMA, A. (1985). Voltage dependence of Na/K pump current in isolated heart cells. *Nature* **315**, 63–65.

GLITSCH, H. G., REUTER, H. & SCHOLZ, H. (1970). The effect of the internal sodium concentration on calcium fluxes in isolated guinea-pig auricles. *Journal of Physiology* **209**, 25–43.

HAMILL, O. P., MARTY, A., NEHER, E., SAKMANN, B. & SIGWORTH, F. J. (1981). Improved patch-clamp techniques for high-resolution current recording from cells and cell-free membrane patches. *Pflügers Archiv* **395**, 6–18.

HILLE, B. (1984). *Ionic Channels of Excitable Membranes*. Sunderland, MA: Sinauer.

KADOMA, M., FROEHLICH, J., REEVES, J. & SUTKO, J. (1982). Kinetics of sodium ion induced calcium ion release in calcium ion loaded cardiac sarcolemmal vesicles: determination of initial velocities by stopped-flow spectrophotometry. *Biochemistry* **21**, 1914–1918.

KASS, R. S., LEDERER, W. J., TSIEN, R. W. & WEINGART, R. (1978). Role of calcium ions in transient inward currents and after-contractions induced by strophanthidin in cardiac Purkinje fibres. *Journal of Physiology* **281**, 187–208.

KIMURA, J., MIYAMAE, S. & NOMA, A. (1986*a*). Isolation of sodium–calcium exchange current in single ventricular cells of guinea-pig. *Journal of Physiology* **371**, 191*P*.

KIMURA, J., NOMA, A. & IRISAWA, H. (1986*b*). Na–Ca exchange current in mammalian heart cells. *Nature* **319**, 596–597.

LANGER, G. A. (1982). Sodium–calcium exchange in the heart. *Annual Review of Physiology* **44**, 435–449.

LEDVORA, R. F. & HEGYVARY, C. (1983). Dependence of Na^+–Ca^{2+} exchange and Ca^{2+}–Ca^{2+} exchange on monovalent cations. *Biochimica et biophysica acta* **729**, 123–136.

MATSUDA, H. & NOMA, A. (1984). Isolation of calcium current and its sensitivity to monovalent cations in dialysed ventricular cells of guinea-pig. *Journal of Physiology* **357**, 553–573.

MULLINS, L. J. (1979). The generation of electric current in cardiac fibers by Na/Ca exchange. *American Journal of Physiology* **236**, C103–110.

MULLINS, L. J. (1981). *Ion Transport in Heart*. New York: Raven Press.

MULLINS, L. J. & BRINLEY JR, F. J. (1975). Sensitivity of calcium efflux from squid axons to changes in membrane potential. *Journal of General Physiology* **65**, 135–152.

NOBLE, D. (1986). Sodium–calcium exchange and its role in generating electric current. In *Cardiac Muscle: Excitation and Regulation of Contraction*, ed. NATHAN, R. D. London: Academic Press (in the Press).

PHILIPSON, K. D. (1985). Sodium–calcium exchange in plasma membrane vesicles. *Annual Review of Physiology* **47**, 561–571.

PITTS, B. J. R. (1979). Stoichiometry of sodium–calcium exchange in cardiac sarcolemmal vesicles: coupling to the sodium pump. *Journal of Biological Chemistry* **254**, 6232–6235.

REEVES, J. P. & HALE, C. C. (1984). The stoichiometry of the cardiac sodium–calcium exchange system. *Journal of Biological Chemistry* **259**, 7733–7739.

REEVES, J. P. & SUTKO, J. L. (1983). Competitive interactions of sodium and calcium with the sodium calcium exchange system of cardiac sarcolemmal vesicles. *Journal of Biological Chemistry* **258**, 3178–3182.

REUTER, H. & SEITZ, N. (1968). The dependence of calcium efflux from cardiac muscle on temperature and external ion composition. *Journal of Physiology* **195**, 451–470.

RUSSELL, J. M. & BLAUSTEIN, M. P. (1974). Calcium efflux from barnacle muscle fibers. *Journal of General Physiology* **63**, 144–167.

SATO, R., NOMA, A., KURACHI, Y. & IRISAWA, H. (1985). Effects of intracellular acidification on membrane currents in ventricular cells of the guinea pig. *Circulation Research* **57**, 553–561.

SCHWARZENBACH, G., SENN, H. & ANDEREGG, G. (1957). Komplexone XXIX. Ein grosser Chelat-effekt besonderer Art. *Helvetica chimica acta* **40**, 1886–1900.

SIEGL, P. K. S., CRAGOE, E. J., TRUMBLE, M. J. & KACZOROWSKI, G. J. (1984). Inhibition of Na^+/Ca^{2+} exchange in membrane vesicle and papillary muscle preparations from guinea pig heart by analogs of amiloride. *Proceedings of the National Academy of Sciences of the U.S.A.* **81**, 3238–3242.

SHEU, S. & FOZZARD, H. (1982). Transmembrane Na^+ and Ca^{2+} electrochemical gradients in cardiac muscle and their relationship to force development. *Journal of General Physiology* **80**, 325–351.

SOEJIMA, M. & NOMA, A. (1984). Mode of regulation of the ACh-sensitive K-channel by the muscarinic receptor in rabbit atrial cells. *Pflügers Archiv* **400**, 424–431.

SULAKHE, P. V. & ST. LOUIS, P. J. (1980). Passive and active calcium fluxes across plasma membranes. *Progress in Biophysics and Molecular Biology* **35**, 135–195.

TANIGUCHI, J., KOKUBUN, S., NOMA, A. & IRISAWA, H. (1981). Spontaneously active cells isolated from the sino-atrial and atrioventricular nodes of the rabbit heart. *Japanese Journal of Physiology* **31**, 547–558.

TIBBITS, G. F. & PHILIPSON, K. D. (1982). Na-dependent alkaline earth metal uptake in cardiac sarcolemmal vesicles. *Federation Proceedings* **41**, 1240.

TSIEN, R. Y. (1980). New calcium indicators and buffers with high selectivity against magnesium

and protons: design, synthesis, and properties of prototype structures. *Biochemistry* **19**, 2396–2404.

TSIEN, R. Y. & RINK, T. J. (1980). Neutral carrier ion-selective microelectrodes for measurement of intracellular free calcium. *Biochimica et biophysica acta* **599**, 623–638.

VAUGHAN-JONES, R. D., LEDERER, W. J. & EISNER, D. A. (1983). Ca^{2+} ions can affect intracellular pH in mammalian cardiac muscle. *Nature* **301**, 522–524.

WIER, W. G. & ISENBERG, G. (1982). Intracellular Ca^{2+} transients in voltage clamped cardiac Purkinje fibers. *Pflügers Archiv* **392**, 284–290.

YAU, K. & NAKATANI, K. (1984). Electrogenic Na–Ca exchange in retinal rod outer segment. *Nature* **311**, 661–663.

YELLEN, G. (1982). Ca-activated non-selective channels in neuroblastoma. *Nature* **296**, 357–359.